$K_2La_6I_{12}Os$: A New Structure Type for Isolated Clusters That Is Generated by Cation Requirements

S. Uma and John D. Corbett*

Department of Chemistry, Iowa State University, Ames, Iowa 50011

Received December 2, 1997

Reaction of KI, La, LaI_3, and Os in a welded niobium tube at 800 °C yields black, air-sensitive crystals of $K_2La_6I_{12}Os$. The phase was characterized by single-crystal X-ray diffraction (monoclinic, $P2_1/c$, $Z = 2$, $a = 9.890(3)$ Å, $b = 19.319(5)$ Å, $c = 10.047(4)$ Å, $\beta = 108.69(3)°$ at 23 °C). The structure contains tetragonally compressed La_6I_{12} clusters centered by Os and interbridged by I^a atoms according to the general pattern of $(R_6Z)I^i_6I^{i-a}_{6/2}I^{a-i}_{6/2}$ for all examples with X:R ratios of 2:1. However, the detailed pattern of three-bonded I^{i-a} and I^{a-i} bridging is new owing to the need to accommodate a relatively large, distorted cluster and two potassium ions in a more open structure. One type of I^{i-a} and I^{a-i} bridging defines zigzag chains of clusters with strain evident in the interconnections. EHMO calculations show that the observed 0.49 Å tetragonal compression of the 16-electron cluster (relative to an optimal 18-e) splits the nominal t_{1u}^4 HOMO into a two-below-one pattern and gives a closed-shell configuration. The compound accordingly exhibits only a small and typical temperature-independent paramagnetism, $\sim 6 \times 10^{-4}$ emu mol^{-1}.

Introduction

The importance of exploratory synthesis in solid state chemistry is well established by the large variety of new compounds with unusual structures and properties that have been discovered. The forecast of phase stability even among a group of definite alternatives remains one of the most elusive problems in solid state science, while the inability to conceive of new structure types seems substantially insuperable at present. This lack of predictability offers great excitement and surprise with the discovery of unknown, even unprecedented compounds.

The chemistry of reduced rare-earth metal (R) cluster halides (especially iodides) in the presence of different interstitial elements is remarkably broad.[1,2] The common structural feature in most of these reduced clusters is the presence of R_6X_{12} units in which the halogen atoms (X) bridge all edges of nominal metal octahedra (R_6) which in turn enclose interstitial atoms Z. Possible interstitial atoms are late transition metals (groups 7−11), main-group elements (Be−N, Si, etc.,), and also small dimers such as C_2. These interstitial atoms provide both central bonding and additional valence electrons for the cluster bonding orbitals and thereby aid in fulfilling the minimal electron counts for bonding of the relatively electron-poor rare-earth metals. The clusters within these compounds may remain either isolated or be condensed into dimers or larger units, depending principally upon the halide:metal ratio. Different structures found for a given ratio further depend on both the connectivities provided by the halide atoms as these interlink the clusters into various different frameworks, and any countercations that may be incorporated.

Our recent exploratory research has been focused on the introduction of alkali-metal atoms into compounds of rare-earth metal-rich cluster compounds in order to examine the nature of quaternary compounds. Although many quaternary cluster compounds are known among reduced zirconium halides,[1] the corresponding isolated rare-earth element clusters were once known only with main-group interstitials in such as $Cs_4Pr_6I_{13}C_2$, $Cs_4Sc_6I_{13}C$,[3] $CsEr_6I_{12}C$,[4] and $Cs_2Pr_6I_{12}C_2$.[5] Earlier attempts toward this goal have been successful with the discovery of the new $Cs_4R_6I_{13}Z$ structure type (R = Ce, Pr; Z = Co, Os) with isolated metal clusters.[6] The novel connectivity here can be formulated as $Cs_4(R_6Z)I^i_8I^{i-a}_{4/2}I^{a-i}_{4/2}I^{a-a}_{2/2}$ in which an I^i atom bridges an edge of the metal octahedron, I^a atoms bond exo at R vertexes, and the other symbols denote bifunctionality. Another structural type $AR_6I_{10}Z$ (A = K, Cs; R = La, Pr; Z = Mn, Fe, Os)[7] has the halide connectivity between clusters $A(R_6Z)I^i_2I^{i-i}_{4/2}I^{i-a}_{6/2}I^{a-i}_{6/2}$ with more multiple functions for fewer halides. Subsequent studies also uncovered the unprecedented bioctahedral rare-earth metal clusters $A_2R_{10}I_{17}Z_2$ (A = Rb, Cs; R = La, Ce, Pr; Z = Co, Ni, Ru, Os) in which the $R_{10}Z_2$ units are sheathed and interbridged by iodine atoms.[8,9] These show the new interconnection pattern $A_2(R_{10}Z_2)I^i_8I^{i-a}_{8/2}I^{a-i}_{8/2}$.

The present article describes another new structure that we have encountered during our extended explorations in metal-rich systems in the presence of alkali metals.

(1) Corbett, J. D. In *Modern Perspectives in Inorganic Crystal Chemistry*; Parthe, E., Ed.; Kluwer Academic Publishers: Dordrecht, The Netherlands, 1992; p 27. (b) Corbett, J. D. *J. Alloys Compd.* **1995**, *224*, 10.
(2) Simon, A.; Mattausch, H.; Miller, G. J.; Bauhofer, W.; Kremer, R. K. In *Handbook on the Physics and Chemistry of Rare Earths*; Gschneider, K. A., Jr., Eyring, L., Eds.; Elsevier Science Publishers B.V.: Amsterdam, 1991; Vol. 15, p 191.
(3) Artelt, H. M.; Meyer, G. *Z. Anorg. Allg. Chem.* **1994**, *620*, 1521.
(4) Artelt, H. M.; Schleid, T.; Meyer, G. *Anorg. Allg. Chem.* **1992**, *618*, 18.
(5) Artelt, H. M.; Meyer, G. *Z. Anorg. Allg. Chem.* **1993**, *619*, 1.
(6) Lulei, M.; Corbett, J. D. *Inorg. Chem.* **1996**, *35*, 4084.
(7) Lulei, M.; Corbett, J. D. *Z. Anorg. Allg. Chem.* **1996**, *622*, 1677.
(8) Lulei, M.; Maggard, P. A.; Corbett, J. D. *Angew. Chem., Int. Ed. Engl.* **1996**, *35*, 1704.
(9) Lulei, M.; Martin, J. D.; Hoistad, L. M.; Corbett, J. D. *J. Am. Chem. Soc.* **1997**, *119*, 513.

S0020-1669(97)01506-1 CCC: $15.00
Published on Web 03/25/1998

Experimental Section

Synthesis. The synthetic and sublimation techniques for LaI_3 and the reaction procedures utilizing welded Nb tubing have been described before.[9−11] KI (Fisher, 99.95%) was dried under dynamic vacuum and then sublimed. La metal (Ames Laboratory) and Os powder (Alfa, 99.95%) were used as received and handled in a glovebox. A reaction with a stoichiometric target $K_2La_6I_{13}Os$ heated at 800 °C for 27 days and slowly cooled at 5 °C/h to 300 °C first produced black crystals of $K_2La_6I_{12}Os$ (∼50% according to the Guinier powder diffraction pattern calculated after the structural solution), 10% LaOI, and an unknown phase which gave a few additional lines. The former phase was also obtained in ∼40% yield (plus 40% $KLa_6I_{10}Os$[7] and 10% LaOI) from reactions with the composition $K_2La_{12}I_{19}Os_2$.

Subsequent reactions under the same reaction conditions with the exact stoichiometry yielded black, microcrystalline samples of $K_2La_6I_{12}$-Os in high yield (∼90%, besides ca. 10% LaOI). Attempts to obtain $Rb_2La_6I_{12}Os$, $Cs_2La_6I_{12}Os$ and $Cs_2Ce_6I_{12}Os$ yielded principally the corresponding $A_2R_{10}I_{17}Os_2$ phases[9] instead. Several reactions with other interstitials and rare-earth elements did not yield any $A_2R_6I_{12}Z$ compounds. Those with $K_2La_6I_{12}Fe$ and $K_2La_6I_{12}Ru$ compositions resulted only in major amounts of $KLa_6I_{10}Fe$[7] and La_3I_3Ru,[12] respectively. Reactions with Mn and Co as interstitials gave unidentified products and so did those with Pr and Ce instead of La.

Single Crystal and X-ray Study. Crystals of $K_2La_6I_{12}Os$ were mounted in thin-walled glass capillaries in the glovebox, and their quality was checked by Laue photographs on Weissenberg cameras. Monoclinic cell parameters and an indication of Laue symmetry 2/*m* were obtained from an approximately 0.05 × 0.05 × 0.20 mm crystal after a least-squares refinement of the setting angles of 25 centered reflections collected on a Rigaku AFC6R diffractometer with the aid of graphite-monochromated Mo Kα radiation. A total of 4754 reflections was collected ($4 \le 2\theta \le 50°$; $\pm h, \pm k, \pm l$; $2\theta-\omega$ scans) at room temperature, and these gave 2483 unique data ($R_{av} = 16.2\%$) for space group $P2_1/c$ (No. 14) of which 815 were observed ($I > 3\sigma_I$). The last was uniquely indicated by the indication of a centrosymmetric space group on the basis of intensity statistics and the systematic absences exhibited by the data set ($h0l$, $l \neq 2n$; $0k0$, $k \neq 2n$).

The structure was solved by direct methods (SHELXS[13]). Programs, scattering factors, etc. were those in the TEXSAN package.[14] An empirical absorption correction ($\mu = 207.8$ cm^{-1}) was applied to the full data set with the aid of three ψ scans at χ near 90° and later, after isotropic refinement, by DIFABS, as recommended[15] (relative transmission coefficient range: 0.851−1.00). The second step consistently reduced the standard deviations, especially for the positional parameters of the iodine atoms. The residuals after the complete anisotropic refinement of all atoms (97 variables, 815 reflections) were $R(F) = 0.042$ and $R_w = 0.038$. The largest residual peak in a ΔF map was 1.52 e/Å^3, 1.6 Å from K.

The Guinier powder pattern calculated for the refined structural model agreed very well with that observed for the bulk product with Si as a common internal standard. This allowed indexing of the pattern and a better determination of the lattice constants. Some data collection and refinement parameters are given in Table 1. The final atomic coordinates, isotropic-equivalent temperature factors, and estimated standard deviations are listed in Table 2. Additional data collection and refinement information and the anisotropic displacement parameters are available as Supporting Information. These and the structure factor data are also available from J.D.C.

Physical Property Measurements. Magnetic susceptibilities of $K_2La_6I_{12}Os$ were measured after loading a 20-mg sample in a He-filled glovebox into an improved fused silica container.[16] The magnetic susceptibilities were measured at 3 T over a range of 6−300 K on a Quantum Design SQUID magnetometer. The magnetization of the sample was first checked as a function of the applied field between 0 and 6 T at 50 and 200 K to screen for possible impurities, but these were found to be ideal ($M(T) \rightarrow 0$ at $H = 0$). The data were corrected for the susceptibility of the container and for the standard diamagnetic core terms.

Calculations. EHMO calculations[17] were carried out for the isolated $La_6(Os)I_{12}I_6^{8-}$ cluster with exo-bonded iodine included. Suitable H_{ii} parameters for La, Os, and I, viz. (in eV) La, 6s, −6.56; 6p, −4.38; 5d, −7.52; Os, 6s, −8.17; 6p, −4.81; 5d, −11.84; I, 5s, −20.8; 5p, −11.2 were taken from charge-consistent interactions on similar compounds.[9,10]

Table 1. Some Crystallographic Data for $K_2La_6I_{12}Os$

fw	2624.66
space group, *Z*	$P2_1/c$ (No. 14), 2
lattice constants[a]	
a (Å)	9.890(3)
b (Å)	19.319(5)
c (Å)	10.047(4)
β (deg)	108.69(3)
V (Å^3)	1818(1)
D_{calc} (g/cm^3)	4.808
μ (Mo Kα, cm^{-1})	207.81
R, R_w[b]	0.042, 0.038

[a] Cell constants refined from Guinier powder pattern reflections measured with Si as internal standard; $\lambda = 1.540\,562$ Å, 23 °C. [b] $R = \sum||F_o| - |F_c||/\sum|F_o|$; $R_w = [\sum w(|F_o| - |F_c|)^2/\sum w(F_o)^2]^{1/2}$; $w = \sigma_F^{-2}$.

Table 2. Positional and Isotropic Equivalent Displacement Parameters (Å^2) for $K_2La_6I_{12}Os$

atom	*x*	*y*	*z*	U_{iso}[a]
Os	0	0	0	0.70(1)
La1	−0.0068(4)	0.0458(2)	0.2748(3)	1.3(1)
La2	0.0234(3)	−0.1459(2)	0.0969(3)	1.4(1)
La3	0.2868(3)	0.0129(2)	0.0910(3)	1.4(1)
I1	0.3680(4)	−0.1449(2)	0.2209(4)	2.6(2)
I2	0.3267(4)	0.0659(2)	0.4088(4)	3.0(2)
I3	−0.3484(4)	0.0306(3)	0.2006(4)	3.1(2)
I4	0.0253(5)	−0.1053(2)	0.4160(4)	3.2(2)
I5	−0.0817(5)	0.2071(2)	0.1887(4)	3.4(2)
I6	0.3113(4)	0.1790(2)	0.0199(5)	3.6(2)
K	−0.426(2)	0.193(1)	0.412(2)	8(1)

[a] $U_{iso} = (8\pi^2/3)\Sigma_i\Sigma_j U_{ij} a_i^* a_j^* \vec{a}_i \vec{a}_j$.

Results and Discussion

Structure. The presence of the large Os interstitial and two relatively small K^+ countercations results in a new monoclinic structure type for $K_2La_6I_{12}Os$, space group $P2_1/c$ ($Z = 2$). Some characteristics of this structure are nominal octahedral metal clusters defined by three crystallographically distinct metal atoms and an enclosed Os atom that lies on an inversion center. The only other symmetry elements are the improper 2_1 screw and *c* glide, and all atoms but Os lie in general positions. Figures 1 and 2 show [001] and [100] views of the bridging about one cluster and a unique set of atom numbers. The twelve edges of the La_6Z cluster are bridged by six crystallographically different iodine atoms to form the well-known R_6X_{12} unit. The range of La−La distances ($\Delta = 0.206(6)$ Å) and the corresponding Os−La separations ($\Delta = 0.269(4)$ Å, Table 3) describe a substantial distortion from octahedral symmetry, a compression along the La3−Os−La3 axis. The genesis of this appears to be concerted effects of an electronic instability of the 16-e cluster (below) and probably also the asymmetry of the intercluster

(10) Hughbanks, T.; Corbett, J. D. *Inorg. Chem.* **1988**, *27*, 2022.
(11) Corbett, J. D. *Inorg. Synth.* **1983**, *22*, 15, 31.
(12) Payne, M. N.; Dorhout, P. K.; Kim, S.-J.; Hughbanks, T. R.; Corbett, J. D. *Inorg. Chem.* **1992**, *31*, 1389.
(13) Sheldrick, G. M. *SHELXS-86*; Universitat Göttingen: Germany, 1986.
(14) *TEXSAN*, Version 6.0; Molecular Structure Corp.: The Woodlands, TX, 1990.
(15) Walker, N.; Stuart, D. *Acta Crystallogr.* **1983**, *A39*, 159.
(16) Guloy, A. M.; Corbett, J. D. *Inorg. Chem.* **1996**, *35*, 4669.
(17) Whangbo, M.-H.; Hoffmann, R. *J. Am. Chem. Soc.* **1978**, *100*, 6093. (b) Ammeter, J. H.; Birgi, H.-B.; Thibeault, J.; Hoffmann, R. *J. Am. Chem. Soc.* **1978**, *100*, 3686.

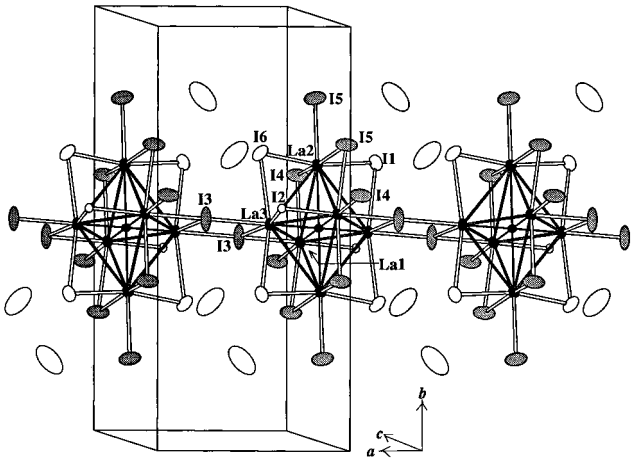

Figure 1. ~[001] view of the individual clusters in $K_2La_6I_{12}Os$ and the intercluster bridging along [100]. Interconnected La and Os atoms in the clusters are shown with solid ellipsoids, bridging I^{i-a} are shaded, and I^i and K have open (90% probability) ellipsoids. Only the unique atoms in the centric clusters are labeled.

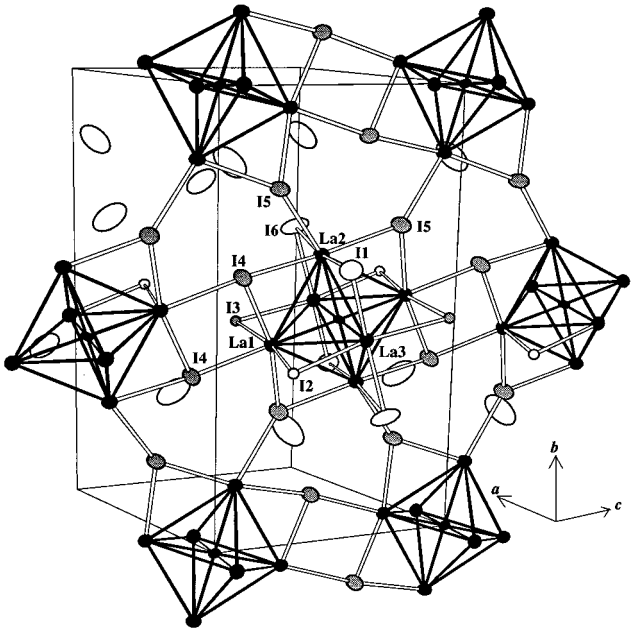

Figure 2. [100] view of the structure of $K_2La_6I_{12}Os$ showing the pairs of I4 bridges to each cluster, the strained, multiple cluster bridging by I5, and the approximately close-packed [100] cluster layer generated.

iodine bridging. The latter is best related in terms of the known alternatives, as follows.

Bonding constraints for all $R_6X_{12}Z$ stoichiometries are the need both to bridge all 12 edges of each cluster (X^i) and to bond X^a exo at the six metal vertexes, which leads to the connectivity $R_6(X^i)_6(X^{i-a})_{6/2}(X^{a-i})_{6/2}$ in which half the halogens are bifunctional. The spatial dispositions of X^i relative to X^{i-a} distinguish among various 6−12 structure types. The parent rhombohedral $Zr_6X_{12}Z$ (Z = Be, B, C, H)[18] is built of layers of centric trigonal-antiprismatic clusters stacked along $\bar{3}$ axes. The six X^{i-a} that lie around the waists of the antiprisms are exo bonded to cluster vertexes in the adjoining layers, and vice versa, waist iodine in the latter bonding in parallel to vertexes of the central cluster. (This complementary functionality can be seen for I3 and I4 in the intercluster rhomboids in Figures 1 and 2, respectively.) The three halogens at each end of the cluster remain X^i. In $Sc_7X_{12}Z$, the antiprismatic $\bar{3}$ sites between clusters pairs defined by the latter X^i accommodate an additional Sc^{III} atom.[10,19]

Table 3. Important Distances (Å) and Angles (deg) in $K_2La_6I_{12}Os$

Os−La1	2.921(3)	I1−K	3.67(2)
Os−La2	2.967(3)	I1−K	3.52(2)
Os−La3	2.698(3)	I2−K	3.46(2)
		I3−K	4.00(2)
La1−La2	4.166(4)	I4−K	4.15(2)
La1−La2	4.162(5)	I5−K	4.12(2)
La1−La3	3.960(4)	I6−K	3.98(2)
La1−La3	3.993(5)	I6−K	3.97(2)
La2−La3	4.038(4)		
La2−La3	3.983(5)		
		I2−I2[b]	4.190(9)
La1−I2	3.162(6)	I4−I5	3.863(6)
La1−I3	3.231(5)		
La1−I4[a]	3.372(5)	Os−La1−I4	177.2(2)
La1−I4	3.218(5)	Os−La2−I5	162.5(1)
La1−I5	3.255(5)	Os−La3−I3	178.9(1)
La2−I1	3.233(5)	I2−La1−I3	168.8(2)
La2−I4	3.294(5)	I4−La1−I5	165.5(1)
La2−I5	3.321(5)	I1−La2−I6	168.9(2)
La2−I5[a]	3.498(5)	I4−La2−I5	167.0(2)
La2−I6	3.202(5)	I1−La3−I6	162.0(1)
La3−I1	3.313(5)	I2−La3−I3	162.9(1)
La3−I2	3.255(6)		
La3−I3	3.287(5)		
La3−I3[a]	3.435(5)		
La3−I6	3.313(5)		

[a] Exo I^{a-i}. [b] d(I−I) < 4.33 Å, all intercluster.

Insertion of the large cation in rhombohedral $CsEr_6I_{12}C$ generates just the reverse bridging arrangement; the parallel I^{i-a}, I^{a-i} bonding functions are disposed around the ends of the antiprism, while the I^i atoms about the waists of the $\bar{3}$ clusters are part of the 12-coordinate sites for Cs^+ that alternate with clusters along $\bar{3}$.[4] On the other hand, pairs of 11-coordinate Cs^+ sites in $Cs_2Pr_6(C_2)I_{12}$ ($P\bar{1}$) are generated with four I^{i-a}, I^{a-i} pairs around the waists of nominal octahedra, two more I^{i-a} lying on other trans edges of the clusters.[5] The present $K_2La_6I_{12}Os$ meets the needs of the larger interstitial and two smaller K^+ counteractions in yet another way. Here pairs of three I^{i-a} connections lie on opposite sides of the centric cluster with a common La1 vertex in each; that is, they bridge three of the four cis edges that meet at La1, I3 on La1−La3 and I4 and I5 on La1−La2 edges (Figures 1 and 2; the I^{i-a} are shaded therein). As usual, the corresponding $I3^{a-i}$ and $I4^{a-i}$ in other clusters form parallel bridges (rhomboids) and are exo to the respective La3 and La1, thus interconnecting the clusters in the [100] and [001] directions. But the disposition of I5 is new and different; the two trans $I5^{i-a}$ connect clusters along [010] while the two $I5^{a-i}$ counterfunctions to La2 involve different clusters (Figure 2). These are seen to be related by horizontal 2_1 screw axes along x, $^1/_4$, 0, etc. and to so generate [100] layers of interbridged, approximately close-packed clusters, but with some distortions.

Each cluster has left a pair of $I1^i$, $I6^i$, and $I2^i$ atoms (unshaded) that bridge four La2−La3 edges about the waist of the octahedron (Figure 2) and a trans pair of La1−La3 edges (Figure 1), respectively. These all have common termini at the La3 vertexes. The 0.49 Å compression of the cluster along La3−Os−La3 is thus associated with La3 vertexes to which three of the more basic I^i are bound, while La1 about the waist has three I^{i-a} neighbors, and La2, two I^{i-a}. We suppose that the slight (0.046 Å) shortening of the cluster along La1−Os−La1 (vs the

(18) Ziebarth, R.; Corbett, J. D. *J. Solid State Chem.* **1989**, *80*, 56.

(19) Dudis, D. S.; Corbett, J. D.; Hwu, S.-J. *Inorg. Chem.* **1986**, *25*, 3434.

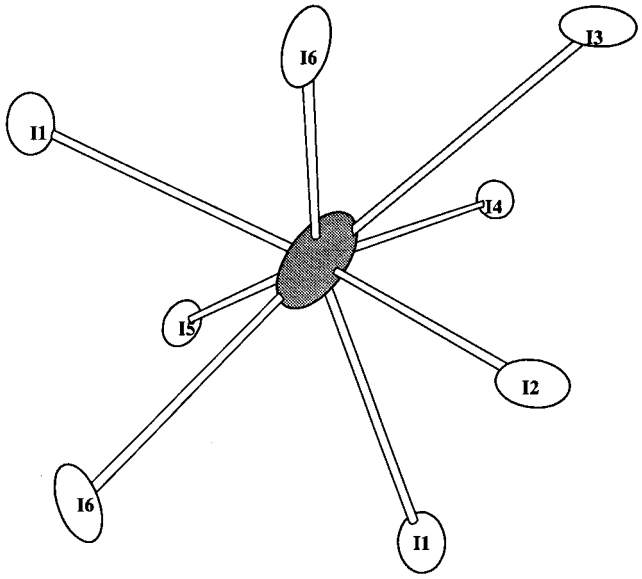

Figure 3. Iodines surrounding the potassium cation, with distances that range from 3.46 to 4.15 Å.

La2 axis) results from the opposite effect of the predominant bonding of the less basic I^{i-a} to La1.

The bridged $K_2La_6I_{12}Os$ structure and cluster distortions are also associated with some evident strain in the lattice. Although "matrix effects" associated with closed-shell X···X contacts, such as X^a riding on the four X^i about each vertex, are common and significant in many cluster networks, such are not important here. Presumably because of the large sizes of Os and La, all intracluster I···I contacts are greater than 4.3 Å vs fairly short contacts of 3.95−4.00 Å found in other iodides. On the other hand, the bridges between three clusters via $I5^{i-a}$ and $I5^{a-i}$ bonded at La2 vertexes are significantly distorted relative to the regular pairs of I3 and I4 double bridges. This is seen in several Os−La2−I5 radial connections in Figure 2 that are bent from a normal 180° to 162.5°. The La2−$I5^a$ distance is also the longest of its type in the structure. These rather awkward I5 bridges also result in unusually short (3.86 Å) I5−I4 contacts between clusters, Figure 2 (across the 2_1 axis at $y = {}^1/_4$).

The coordination sphere of the less demanding potassium counterion is irregular, Figure 3. The cation is surrounded by eight iodine atoms over a range of 0.69 Å, with an average, 3.858 Å, that is 0.15 Å greater than the sum of Shannon radii.[20] These circumstances are presumably reflected in the large and irregular thermal ellipsoids for potassium (Table 2). Many examples are known in other quaternary cluster halides in which like cations lie in poorly defined, low-symmetry sites.[1,7,21] Alkali-metal atoms often mainly fulfill charge requirements, while the dominant framework is formed by the clusters and the bridging halides.

Calculations. The contributions of main-group or transition-element interstitials to the bonding and stabilization of isolated, octahedral rare-earth element[10,22,23] and zirconium clusters[24−26] have been discussed in detail on the basis of extended Hückel molecular orbital calculations. The interstitial elements provide

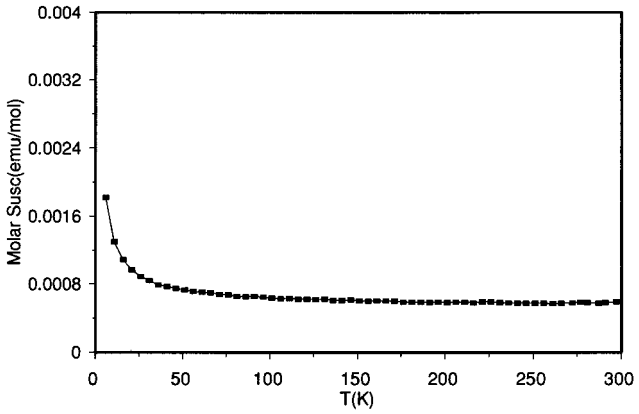

Figure 4. Molar magnetic susceptibility of $K_2La_6I_{12}Os$, corrected for core diamagnetism.

both electrons and orbitals for the formation of strong bonds with the cluster skeleton. Eighteen electrons are optimal for nominally octahedral 6−12 type clusters that are centered by transition elements, corresponding to the R−Z bonding $a_{1g}^2\ t_{2g}^6$, the R−R bonding HOMO t_{1u}^6, and the nominally nonbonding e_g^4 orbitals on Z. The 16-electron cluster in $K_2La_6I_{12}Os$ shows a compression of 0.49 Å along La3−Os−La3 relative to the average of the other two axes (Table 3). Similar tetragonal compressions have been observed for the 16-electron clusters in $Y_6I_{10}Ru$ (0.41 Å)[10] and $Pr_6Br_{10}Ru$ (0.55 Å)[27] but notably less (0.18 Å) in $Y_6I_{10}Os$.[10,28] Relatively little distortion is observed in the 17-electron example $Pr_6Br_{10}Co$ (0.24 Å)[27] and actually a small expansion in $Y_6I_{10}Ir$.[28] Extended Hückel MO calculations on $Y_6I_{10}Ru$[10] indicated that interactions between 4d orbitals on the Y atoms cause a 0.30 eV splitting of the nominal t_{1u}^4 HOMO into a counterintuitive two-below-one ($e_u(x,y)$ and $b_{2g}(z)$) pattern, mostly because the Ru 5p levels lie too high to be effective in Y−Ru bonding. A similar result was obtained for $Pr_6Br_{10}Ru$[27] where the surprisingly greater axial compression (0.55 Å) was attributed to reduced matrix effects caused by the larger Pr and smaller bromide. Relativistic effects were imagined to be responsible for the smaller distortion in $Y_6I_{10}Os$ and $Y_6I_{10}Ir$,[28] but this certainly does not carry over to the present Os-centered phase. Our comparable calculations on a D_{4h} $La_6(Os)I_{12}I_6^{8-}$ cluster also generate two-below-one splitting of t_{1u}^4 HOMO but with a smaller gap (∼0.14 eV) than that earlier calculations on Y−I−Ru and Pr−Br−Ru examples.

The absence of Curie−Weiss behavior for the magnetic susceptibility of $K_2La_6I_{12}Os$ (Figure 4) and the implied closed-shell configuration are quite consistent with the calculations. The observed temperature-independent paramagnetism, $\sim 6 \times 10^{-4}$ emu mol^{-1} after core corrections, however, is comparable to values found for several other rare-earth metal and zirconium cluster halides.[29]

The synthesis of $K_2La_6I_{12}Os$ with the common $R_6X_{12}Z$ cluster composition but a different structure shows how the introduction of alkali metals and suitable Z can lead to new compounds stabilized by transition metals. The compound achieved also illustrates another way in which structures may adapt to meet the necessary bonding and electronic requirements. At the same time, the present structure would appear to mark something near the boundaries of practicality and stability in terms of strain and complexity. The creation of large superstructures, as

(20) Shannon, R. D. *Acta Crystallogr.* **1976**, *A32*, 751.
(21) Ziebarth, R.; Corbett, J. D. *Acc. Chem. Res.* **1989**, *22*, 256.
(22) Hwu, S.-J.; Corbett, J. D. *J. Solid State Chem.* **1986**, *64*, 331.
(23) Hughbanks, T.; Corbett, J. D. *Inorg. Chem.* **1989**, *28*, 631.
(24) Smith, J. D.; Corbett, J. D. *J. Am. Chem. Soc.* **1985**, *107*, 5704.
(25) Smith, J. D.; Corbett, J. D. *J. Am. Chem. Soc.* **1986**, *108*, 1927.
(26) Hughbanks, T.; Rosenthal, G.; Corbett, J. D. *J. Am. Chem. Soc.* **1988**, *110*, 1511.
(27) Llusar, R.; Corbett, J. D. *Inorg. Chem.* **1994**, *33*, 849.
(28) Payne, M. W.; Corbett, J. D. *Inorg. Chem.* **1990**, *29*, 2246.
(29) Steinwand, S. J.; Corbett, J. D. *Inorg. Chem.* **1996**, *35*, 7056.

recently found in $La_6Br_{10}Os$,[30] represents another way in which phase stability may be achieved. Presumably, structural simplicity reflects greater stability in the presence of the same alternative structures.

Acknowledgment. We thank J. E. Ostenson for the magnetic data. This research was supported by the National Science Foundation, Solid State Chemistry, with Grant DMR-9510278, and was carried out in the facilities of the Ames Laboratory, U.S. Department of Energy.

(30) Hong, S.-T.; Hoistad, L. M.; Corbett, J. D. *Inorg. Chem.*, to be submitted.

Supporting Information Available: Two tables with more crystallographic data and anisotropic displacement parameters (2 pages). Ordering information is given on any current masthead page.

IC971506U